I&EC research
Industrial & Engineering Chemistry Research

Article

Cite This: Ind. Eng. Chem. Res. XXXX, XXX, XXX-XXX

pubs.acs.org/IECR

Once-through Circulating Fluidized Bed Boiler Control Design with the Dynamic Relative Gain Array and Partial Relative Gain

Matias Hultgren,*,‡ Enso Ikonen, and Jenő Kovács

Systems Engineering, University of Oulu, POB 4300, Oulun yliopisto, FI-90014, Finland

Supporting Information

ABSTRACT: Combustion power plants currently face major performance challenges, which require robust control design methods. Extensive relative gain analysis was conducted in this paper to generate plantwide control structures for a full-scale once-through circulating fluidized bed boiler. No such study has been reported before for steam boilers. The partial relative gain was employed to generate decentralized control structures based on integral controllability with integrity. The approach provided feasible control structures and verified that basic turbine-following boiler control is preferable in terms of controllability. The steady-state results were extended with the dynamic relative gain array for higher frequencies, which revealed that boiler-following control becomes feasible for faster disturbances. The results highlight the complex interactions between steam pressure and output electrical power control, as well as the loop interactions caused by the feedwater flow in the once-through steam path.

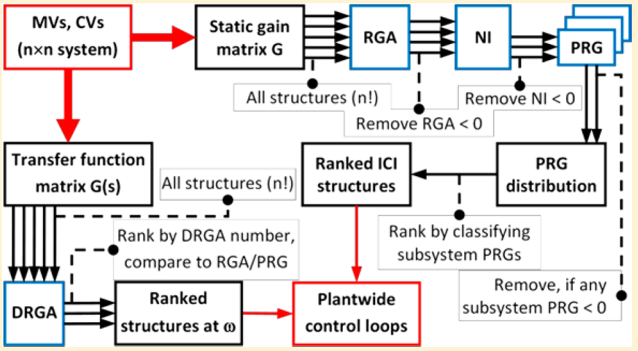

1. INTRODUCTION

This work applies relative gain analysis to once-through circulating fluidized bed (OTU-CFB) boiler plantwide control design. The steam power plant is a complex process with interacting control tasks.[1−3] The steam and combustion sides have different time constant magnitudes, and heat exchangers are located at different positions in the boiler. Dynamics and control are important because of increasing demands for operational flexibility and efficiency. Large boilers are increasingly used for variable loads and fast load transitions with accurate set point tracking demands instead of base load operation. Flowsheets are heavily interconnected, and plants are run close to their operational boundaries. Increased boiler sizes and technologies such as carbon capture and storage (CCS) have also introduced new design requirements for fluidized beds.[4−6]

The new requirements call for advanced design approaches to obtain improved output power responses (Figure 1). First, a deeper interaction between process and control design is needed. In integrated control and process design (ICPD), the two design stages take place simultaneously so that their specific requirements can influence each other.[7] Second, control design should be conducted on a plantwide scale to ensure an effective operation of the whole process.[8] While multivariable dynamic (model predictive) control is rarely feasible on a plantwide level, a more practiced approach is the pairing/decoupling of inputs and outputs into control loops using dedicated selection procedures. Moreover, methods for analyzing system behavior are needed in both plantwide control and ICPD. Relative gain analysis is used in this paper for these purposes.

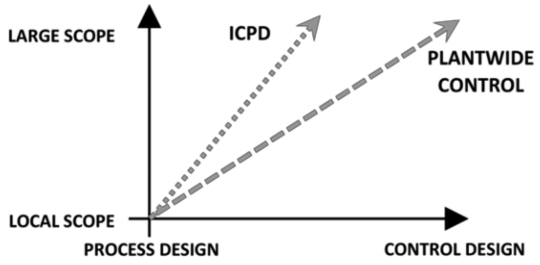

Figure 1. Process and control design directions that aim at improved overall performance of large process systems: plantwide control and integrated control and process design (ICPD).

Relative gain based design is well suited for evaluating controllability and interactions for processes with multiple inputs and outputs,[9,10] such as the OTU-CFB. Another advantage is that closed-loop properties can be determined on the basis of open-loop data, which is useful especially in ICPD.[11] Relative gain analysis is based on the relative gain array, RGA.[12] Modifications of the RGA include the dynamic RGA (DRGA) and the partial relative gain (PRG). The DRGA investigates interactions at higher frequencies,[10,13] while the PRG considers partially controlled systems[14] and can be used as a condition for integral controllability with integrity (ICI).[15,16] While the RGA and the DRGA are established methods, the PRG is featured in few publications.

Received: August 6, 2017
Revised: September 24, 2017
Accepted: November 11, 2017
Published: November 12, 2017

DOI: 10.1021/acs.iecr.7b03259
Ind. Eng. Chem. Res. XXXX, XXX, XXX−XXX

The purpose of this work is to study the PRG and DRGA as tools for controllability analysis and plantwide control design in the OTU-CFB, with potential application to ICPD at a later stage. By evaluating interactions related to specific control connections, this approach can lead to improved electrical power (MW_e) responses. The contribution of this paper is 2-fold. First, systematic plantwide control structure selection is performed for a full industrial OTU-CFB boiler. Only a few studies on plantwide power plant control have been reported in the literature. Niva et al.[17] applied the self-optimizing approach of Skogestad[18] to an oxy-fired CFB pilot. Prasad et al.[19] used centralized model predictive control for a drum boiler, while Garduno-Ramirez and Lee[20] combined loop decoupling methods in drum boiler plantwide operation. Notably, existing studies focus on drum boilers, which have a different control setup compared to the OTU.

The second contribution is that extensive controllability and interaction analysis is performed for the entire CFB boiler using the DRGA and the PRG, which has not been done before. The steady-state RGA has been used to some extent,[21−23] commonly for the 3 × 3 input−output Åström-Bell drum boiler model.[20,24] For example, the block relative gain was also used for a 4 × 4 furnace temperature control problem by Manousiouthakis et al.[25] Unlike the existing papers, the present work not only addresses the control structure selection in a large 8 × 8 system, but also aims at analyzing the OTU-CFB to provide reasons for reduced controllability. The focus is on current OTU-CFB layouts, but the paper also serves as an evaluation of the chosen methods for future flowsheets, which may differ from current designs (e.g., combined heat and solar power). Similarly, relative gain analysis can also be used to uncover unconventional control connections.

The paper is structured as follows. Chapter 2 introduces the OTU-CFB and its main control tasks. Chapter 3 discusses plantwide control design and controllability analysis with the DRGA and PRG methods. Chapter 4 presents the industrial OTU-CFB design case. Chapter 5 shows the results of the PRG and DRGA analysis, and chapter 6 gives the conclusions of the work.

2. THE OTU-CFB PROCESS AND CONTROL

The circulating fluidized bed (CFB) combustion technology[3,26,27] and the once-through (OTU) steam cycle[1,2] are well-known on their own, but the first industrial scale supercritical OTU-CFB was only constructed in 2009.[28,29] CFB boilers enable flexible cocombustion of different fuels and reduced solid fuel emissions. The OTU water-steam setup is the most viable steam cycle for constructing large boilers with fast output power responses, but it is also challenging to control.

2.1. OTU-CFB Process. In a fluidized bed boiler, fuel particles are combusted in a bed of incombustible material. The bed is fluidized by the input oxidant gas flows (primary and secondary). In the CFB setup (Figure 2), particles are entrained with the gas and leave the furnace from the top. Solids are separated from the flue gas in a cyclone and circulated back to the furnace, while the flue gas goes to the backpass duct. Heat exchangers are located in the CFB hotloop and the backpass. The oxidant gas is typically air, but can also be formed in other ways (e.g., oxy combustion).[4−6,30−33]

The steam cycle consists of preheating, evaporation, superheating, expansion, and condensing stages. Feedwater is evaporated in the furnace evaporator and the steam temperature is elevated in the superheating section. This "main steam"

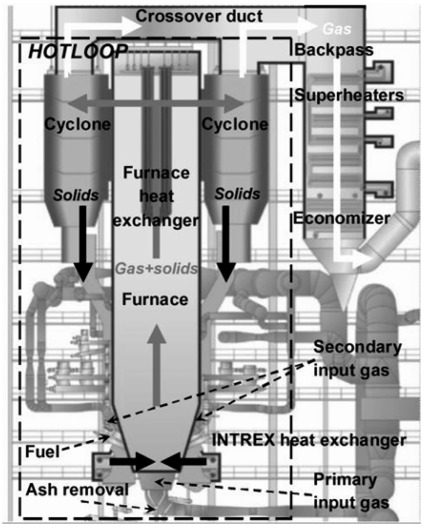

Figure 2. Operational schematic figure of an OTU-CFB, modified from Sumitomo SHI FW.

expands in the turbine, often in several stages with reheating between them. Boilers are classified into drum and once-through units. In drum boilers, water is separated from steam after the evaporator in a drum and circulated back to the evaporator. In OTU boilers, water transforms directly into main steam in a "once-through" pass, and as there is no steam separation stage, the boundaries between preheating, evaporation, and superheating may shift. This setup enables the use of supercritical and sliding-pressure operation, which facilitates the construction of large and efficient boilers with short startup times.

2.2. Main Control Tasks. The control objectives of a power plant can be divided into those related to the steam at the turbine, and those related to efficiency and safety state variables.[1,2,4] The main objectives are to maximize boiler efficiency and to maintain the generated power at its set point, that is, electrical megawatts (MW_e) for condensing plants and heat/electrical power for cogeneration plants. Set point tracking is emphasized in order to follow load demand changes accurately, but disturbance rejection becomes more important for boilers that are primarily run on base load.

2.2.1. Unit Master Control. Unit master control is an upper-level strategy for coordinating steam pressure and output MW_e control. The main setups are boiler-following and turbine-following control (Figure 3).

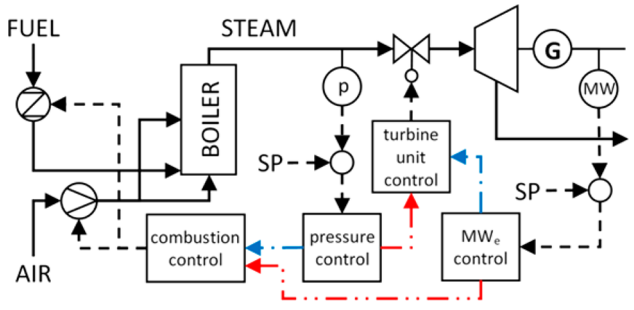

Figure 3. Unit master concepts: turbine-following (red) and boiler-following (blue) control.

In boiler-following control, the MW_e is controlled with the turbine throttle valve and the pressure with the combustion power (fuel and oxidant). A change in the load demand alters

DOI: 10.1021/acs.iecr.7b03259
Ind. Eng. Chem. Res. XXXX, XXX, XXX−XXX

the valve position, and the resulting pressure disturbance is compensated with the combustion power. In turbine-following control, the pressure is controlled with the turbine valve and the MW_e with the combustion power. The heat generation changes according to the load demand and the steam flow is altered to adjust the pressure, which results in an output MW_e change.

2.2.2. Feedwater Control. Feedwater flow rate control is required in order to make up for formed steam. In drum boilers, this largely translates into drum water level control. In OTU boilers, feedwater affects the steam generation directly, which is why mildly superheated steam properties are usually controlled.

2.2.3. Steam Temperature Control. Superheating takes place in a block of superheater (SH) heat exchangers. The main steam (live steam) temperature is regulated between these stages with water sprays from the feedwater line (desuperheaters, DSH), usually with cascade control structures (temperature before and after the spray). The spray water also appears as a steam flow disturbance.

2.2.4. Main Steam Pressure Control. The main steam pressure before the turbine valve is regulated. The pressure can be modified either by changing the turbine valve position or by increasing the steam generation (heat and feedwater). One design factor is whether the pressure is controlled to be constant (constant pressure mode) or whether it is allowed to change with the load level (sliding-pressure mode).

2.2.5. Combustion Control. Combustion control concerns the regulation of the fuel and the oxidant gas, with set points coming from the unit master control. Flue gas O_2 control is included to ensure a sufficient O_2 supply. In CFB boilers, a major requirement is also to maintain the fluidization of the solids. The combustion presents many sources for disturbances, which may require state estimation.[34]

2.2.6. Turbine-Generator Unit Control. Turbogenerator control consists of power, voltage, and frequency control. The generated MW_e depends on the combustion heat and the feedwater, but momentary changes can be made with the turbine valve. Frequency control can be achieved as a cascade structure with the MW_e control.

The OTU boiler is challenging to control. Flow conditions are complex, as water and steam are not separated at a fixed boundary. Thus, there is a direct connection between the evaporation and superheating stages, which leads to strong interactions between steam pressure, steam temperature, and feedwater control. The small OTU storage capacity reduces the possibilities for load disturbance rejection, and combustion disturbances are easily carried over to the steam properties. The high pressures and temperatures in supercritical boilers also lead to small control tolerance limits. All of these factors call for tight control and improved feedforward action.

3. PLANTWIDE CONTROL AND CONTROL PERFORMANCE

Plantwide control provides a control solution for the entire process with good performance and stability, when considering plant dynamics, constraints, disturbances, and control law.[8,18,35] Plantwide design typically employs decentralized control with conventional controllers, such as PID or low-dimensional MIMO (multiple input−multiple output) controllers. Plantwide methods provide the manipulated (MV) and controlled variables (CV) and their pairing into control loops.

3.1. Variable Selections and Performance Evaluation. Process degrees of freedom (DOF) analysis is conducted to determine the amount of MVs for managing CVs. The control degrees of freedom (CDOF)[7,36] should especially be considered, for example, by analyzing the flowsheet one process unit at a time and comparing the total amount of streams (material and energy) to the number of streams that are restrained (e.g., one stream in a mixer) or redundant from being manipulated (e.g., pressures of process units in series), eq 1.[37]

$$\mathrm{CDOF} = N_{\mathrm{total}} - \sum_{\mathrm{units}} (N_{\mathrm{restrained}} + N_{\mathrm{redundant}}) \tag{1}$$

where N_{total}, $N_{\mathrm{restrained}}$, and $N_{\mathrm{redundant}}$ are the amounts of total, restrained, and redundant streams.

MVs, CVs, and measurements are selected systematically based on the DOF, constraints, and steady-state economic optimization.[18] Active constraints and process stabilization should be considered when selecting CVs, and MVs should have favorable static and dynamic qualities. One MV can be designated as the throughput manipulator (TPM), that is, the DOF used to regulate the throughput in the primary process path, from the feed streams to the products.[38,39] The TPM sets the overall production rate, and inventory control should radiate outward from the TPM.

A central question of plantwide control and ICPD is the selection of criteria for describing desirable system behavior.[7] One such criterion is controllability, that is, the ability of the process to achieve and maintain a desired equilibrium. Controllability can be defined in various ways,[10,40,41] such as integral controllability with integrity (ICI).[15,16] A system is ICI controllable if it remains stable, when control loops with integral action are arbitrarily opened and closed or when all loop gains are detuned by the same factor (0−1). Decentralized integral controllability (DIC) is similar to the ICI, but it also demands that the loop gains can be detuned by individual factors.

3.2. Relative Gain Analysis. Relative gain analysis can be used for examining loop interactions, controllability, robustness, and open-loop stability[10] in the OTU-CFB flowsheet. All relative gain methods are variations of the basic relative gain array (RGA).[12] RGA modifications include the performance-RGA (control performance and one-way coupling),[10] the block relative gain (connections between blocks of MVs and CVs),[16,25] the effective RGA (combines RGA with bandwidth or crossover frequencies),[42] and the partial relative gain (PRG),[14] which is discussed in section 3.2.2.

3.2.1. RGA and DRGA. The RGA is calculated with eq 2 from the open-loop steady-state process gain matrix **G**.

$$\mathrm{RGA}(\mathbf{G}) = \mathbf{G} \times (\mathbf{G}^{-1})^{\mathrm{T}} = \begin{bmatrix} \lambda_{11} & \cdots & \lambda_{1n} \\ \vdots & \ddots & \vdots \\ \lambda_{m1} & \cdots & \lambda_{mn} \end{bmatrix} \tag{2}$$

where **G** is the gain matrix, λ_{mn} are relative gains, and "×" is element-by-element multiplication.

Equation 2 applies to square matrices with an equal amount of MVs and CVs, but it has also been modified for nonsquare ones.[43] The RGA contains interaction terms for all single input−single output (SISO) pairings in the system, it is scaling invariant and forms row/column sums of ones. An RGA element signifies the ratio of the open-loop gain for a variable

DOI: 10.1021/acs.iecr.7b03259
Ind. Eng. Chem. Res. XXXX, XXX, XXX−XXX

pairing when all other control loops are open ($g_{OL,OL}$) to the gain when the other loops are closed ($g_{OL,CL}$), eq 3.

$$\lambda_{mn} = \frac{g_{OL,OL}}{g_{OL,CL}} = \frac{(\partial y_m/\partial u_n)_{OL,OL}}{(\partial y_m/\partial u_n)_{OL,CL}} \tag{3}$$

where g is a gain, y is an output, u is an input, n are input indices, and m are output indices.

The RGA can be used for selecting control MV−CV pairings so that interacting effects from other loops on $g_{OL,OL}$ are small. Thus, pairings with λ_{mn} close to 1 are good, and negative λ_{mn} are to be avoided due to instability caused by gain sign change. However, $\lambda_{mn} = 0$ is not conclusive in itself.[14] Small positive λ_{mn} values, usually below 0.5 or even 0.67, are poor (gain increase when closing loops).[9,44] For λ_{mn} larger than 1, interactions dampen the open-loop gain, which requires attention during control (gain increase when opening loops). Very large λ_{mn} values, commonly above 10, require large controller gains and may signify an ill-conditioned system.[44−46]

The dynamic RGA (DRGA), eq 4, extends the (zero frequency) RGA by applying eq 2 to the MV−CV frequency response matrix,[10,11,13] for example, eq 5.[47] The complex DRGA elements are commonly presented as absolute values. Frequency domain investigations are important, as different frequencies might result in different preferred control variable pairings.[42,48]

$$\mathrm{DRGA}(\mathbf{H}(j\omega)) = \mathbf{H}(j\omega) \times (\mathbf{H}(j\omega)^{-1})^{\mathrm{T}} = \begin{bmatrix} a_{\lambda 11} + b_{\lambda 11}j & \cdots & a_{\lambda 1n} + b_{\lambda 1n}j \\ \vdots & \ddots & \vdots \\ a_{\lambda m1} + b_{\lambda m1}j & \cdots & b_{\lambda mn} + b_{\lambda mn}j \end{bmatrix} \tag{4}$$

$$\mathbf{H}(j\omega) = \mathbf{D} + \mathbf{C}(j\omega\mathbf{I} - \mathbf{A})^{-1}\mathbf{B} \tag{5}$$

where $\mathbf{H}(j\omega)$ is the frequency response at frequencies ω (rad/s), a and b are the real and complex terms of the DRGA elements λ_{mn}, and $\mathbf{A}$, $\mathbf{B}$, $\mathbf{C}$, and $\mathbf{D}$ are matrices in a standard state space format.

Control solution ranking can be simplified by using the RGA number,[10] which can also be applied to the DRGA, i.e. nDRGA in eq 6. In the nDRGA, the DRGA with chosen MV−CV pairs on the diagonal is compared to the identity matrix $\mathbf{I}$. As such, a small nDRGA is preferable.

$$\mathrm{nDRGA}(\mathbf{H}(j\omega)) = \| \mathrm{DRGA}(\mathbf{H}(j\omega)) - \mathbf{I} \|_{\mathrm{N}} \tag{6}$$

where "N" is a norm, usually an absolute sum. In this work, "N" is the sum of diagonal elements.

The RGA is often used together with the Niederlinski index (NI), eq 7. The NI denotes the stability of variable pairings: a NI value below zero indicates an unstable system.[14,16] If the MV− CV pairings are located on the diagonal of $\mathbf{G}$, the denominator in eq 7 is simplified to $\prod_i g_{ii}$.

$$\mathrm{NI} = \det(\mathbf{G})/\det(\hat{\mathbf{G}}) \tag{7}$$

where $\hat{\mathbf{G}}$ is the matrix obtained by setting to zero all elements of gain matrix $\mathbf{G}$ that do not correspond to an input−output pairing in a given block-decentralized control structure.

3.2.2. Partial Relative Gain. A downside of the RGA is that it might be misleading for large MV−CV systems because of RGA element changes during partial control. In partially controlled systems, only certain outputs with objectives are controlled, for example, when control systems are designed hierarchically or when some outputs are only controlled indirectly.[10] This can be remedied with the partial relative gain (PRG),[14] which is why it was chosen for the large OTU-CFB system matrices of this work.

The PRG of a partially controlled subsystem, eq 8, is calculated by applying eq 2 to the subsystem gain matrix $\bar{\mathbf{G}}_{mn}$. Gains $\bar{\mathbf{G}}_{mn}$ can be obtained with eq 9. When CV−MV pairings "c" are closed and perfect integral control is assumed, outputs y_c can be controlled to zero.

$$\mathrm{PRG}_{mn}(\mathbf{G}) = \mathrm{RGA}(\bar{\mathbf{G}}_{mn}) = \bar{\mathbf{G}}_{mn} \times (\bar{\mathbf{G}}_{mn}^{-1})^{\mathrm{T}} \tag{8}$$

$$\bar{\mathbf{G}}_{mn} = \mathbf{G}(y_o, u_o) - \mathbf{G}(y_o, u_c)\cdot\mathbf{G}(y_c, u_c)^{-1}\cdot\mathbf{G}(y_c, u_o) \tag{9}$$

where PRG_{mn} is the subsystem PRG, $\bar{\mathbf{G}}_{mn}$ is the modified subsystem gain matrix with loops y_c−u_c closed under integral control, and "o" denotes open loops (CV and MV indices "m" and "n").

The PRG is useful as a condition for ICI controllability.[14] A system $\mathbf{G}$ (size $k \times k$, MV−CV pairs on the diagonal) is ICI if and only if all diagonal RGA elements and the diagonal PRG elements of all partially controlled subsystems ($l \times l$, l = 2, 3,..., $k - 1$) are positive. If NI is also positive, 2 × 2 subsystems need not be checked. ICI controllability is a useful property for multiloop control, as it enables individual controller tuning without introducing instability in the plantwide system.

4. OTU-CFB RELATIVE GAIN ANALYSIS TEST SETUP

This section sets up the PRG and the DRGA analysis for an industrial OTU-CFB condensing power plant in the range of several hundred MW_e (Figure 4). The ICI controllability criterion is specifically tested to determine, whether it offers any advantage for the OTU-CFB. The target of the design is to form feasible control structures between the main process inputs and outputs.

4.1. Model. The investigated large scale OTU-CFB uses a supercritical Benson cycle consisting of an economizer preheater, evaporator water-walls, a four-stage superheating block, three DSH sprays and a reheater. The CFB has a standard hotloop configuration and includes Intrex solid material heat exchangers. The boiler utilizes one coal fuel fraction. Since the focus of the investigation is on the product steam, the condenser is not included in the study.

The power plant was simulated with an extensively validated dynamic model of Sumitomo SHI FW.[29] The simulator is implemented in APROS[49] and consists of standard process unit submodels that are arranged to form the boiler flowsheet. Flowsheet and component dimensions, boundary conditions, and model state values are obtained from steady-state in-house design data.

The thermal hydraulics modeling considers the conservation of mass, momentum, and energy for the supercritical water-steam phase.[50] Heat transfer and wall friction correlations are selected based on wall temperature, saturation temperature, critical heat flux, and minimum film boiling temperature. The solution is based on a staggered grid discretization, where mass and energy equations are solved in the middle of the mesh and momentum equations at the control volume borders. Process units contain control volumes for inlet, outlet, and relevant bulk regions.

The CFB hotloop is modeled using a 1-D Matlab/Simulink CFB block, and this submodel is interfaced with the steam and flue gas path model in APROS. The model utilizes both physical first-principles modeling and empirical correlations.[4,33] The furnace, separator, and Intrex heat exchanger are modeled as units with ideally mixed calculation elements.

4.2. Process Inputs and Outputs. The APROS model was used for the OTU-CFB relative gain analysis. The control degrees

DOI: 10.1021/acs.iecr.7b03259
Ind. Eng. Chem. Res. XXXX, XXX, XXX−XXX

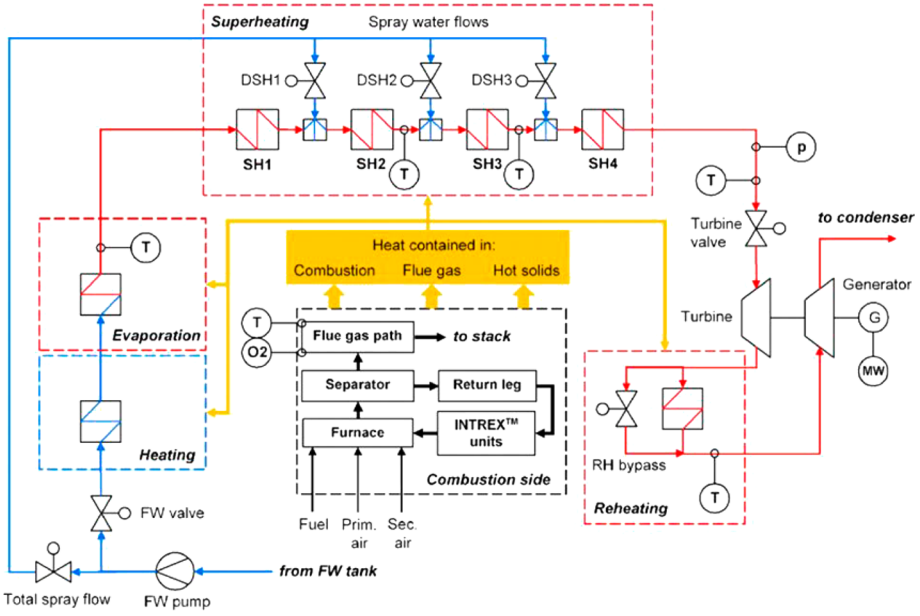

Figure 4. Flowsheet of the OTU-CFB boiler. Feedwater (FW) is marked in blue, steam flows in red, heat transfer in yellow. SH = superheater, DSH = desuperheater, RH = reheater.

of freedom (CDOF) were determined, and open-loop step tests were conducted. Step response data for selected CVs was used to form steady-state gain matrix and transfer function models.

4.2.1. Degrees of Freedom and TPM Considerations. The CFB combustion side (Figure 4) contains five adjustable flows: the fuel, the primary air, the secondary air, the solid material circulation rate, and the flue gas flow. The flue gas flow and circulation rate MVs are limited by furnace pressure and bed inventory safety constraints. The inputs to the steam channel are the feedwater flow to the evaporator and the total DSH flow, which both come from the feedwater line. The steam flow can be adjusted with the feedwater or the turbine valve. The total spray water is split between the three DSH nozzles. A further control possibility is to regulate the steam flow in the reheater, using a bypass with a control valve.

The CDOF is calculated with eq 1 by analyzing each process unit and combining the results into the total CDOF. Considering safety constraints, 42 mass/energy streams can be counted in total, 29 in the steam path, and 13 on the combustion/flue gas side. On the basis of the amount of mass balances without inventories, the steam side has 18 restrained streams (valves, turbines, mixers, feedwater pump, preheater) and the combustion side has 5 (heat exchangers). Pressure control results in redundancy in the steam path and the flue gas duct, and the system heat exchangers thus contain 10 redundant streams. This results in a CDOF of $(29 + 13) - (18 + 5) - 10 = 9$. The independent inputs of the boiler can be selected for example, according to Table 1.

The electrical power at the turbine depends both on the steam flow and the energy content of the steam. The overall MW_e control target thus translates into a steady-state set point for the heat generation through combustion. Three process inputs can be used to adjust the MW_e output, and one of these MVs is available as the boiler throughput manipulator.

- turbine valve: steam volume flow change, transient mass flow change.
- feedwater flow: steam mass flow change, change in energy content (constant fuel firing).

Table 1. Independent MVs of the OTU-CFB Boiler[a]

variable (steam side)	abbreviation	variable (combustion side)	abbreviation
feedwater flow to evaporator	FW	fuel flow to furnace	Fuel
turbine valve position	T.valve	secondary air to furnace	Sec air
desuperheater 1 spray flow	DSH1	primary air to furnace	Prim air
desuperheater 2 spray flow	DSH2		
desuperheater 3 spray flow	DSH3		
reheater bypass valve position	RHvalve		

[a]The primary air flow can basically be treated as a CDOF, although it is also partly bounded by the need to maintain the fluidization.

- fuel and air flows: steam energy content change, no mass flow change (constant FW flow).

In boiler-following control, the TPM is located at the product stream, as the valve can alter the MW_e output quickly. In turbine-following control, the MW_e is modified by the steam generation, that is, the TPM is at the process feed. Steam generation is altered slowly with the fuel firing power, but in theory, the feedwater flow could also be used. No CDOF was specifically designated as the TPM in this work, as the analysis was not limited to any predetermined unit master setup. The OTU cycle also does not directly translate into a traditional inventory control problem.

Twelve MVs were selected for the study, consisting of all MVs from Table 1 and three "combined" MVs (several inputs altered with the same percentage): "total DSH flow" (DSH1, DSH2, and DSH3), "firing power" (fuel and air) and "boiler load" (fuel, air, and feedwater). CVs were selected based on control goals and constraints: main steam pressure and temperature, steam temperature after the evaporator, steam temperatures after superheaters 2–3, steam temperature after the reheater, flue gas (FG) O_2 percentage and temperature, and total output MW_e.

4.2.2. Test Setup and RGA Modeling. On the basis of the CDOF, four square system case studies were constructed to

DOI: 10.1021/acs.iecr.7b03259
Ind. Eng. Chem. Res. XXXX, XXX, XXX−XXX

Table 2. Case Studies 1−4, MV−CV Groups That Are Considered for the OTU-CFB Analysis

var.	inputs	outputs	var.	inputs	outputs
	Case 1			Case 2	
1	T.valve	steam pressure	1	T.valve	steam pressure
2	total DSH	steam temp	2	DSH1 flow	steam temp
3	boiler load	total MW_e	3	DSH2 flow	temp SH2
			4	DSH3 flow	temp SH3
			5	boiler load	total MW_e
	Case 3			Case 4	
1	T.valve	steam pressure	1	T.valve	steam pressure
2	FW flow	steam temp	2	FW flow	steam temp
3	fuel flow	evap. temp	3	Sec air flow	evap. temp
4	Prim air flow	flue gas O_2	4	DSH1 flow	flue gas O_2
5	Sec air flow	flue gas temp	5	DSH2 flow	temp SH2
6	total DSH	total MW_e	6	DSH3 flow	temp SH3
			7	RHvalve	RH temp
			8	firing power	total MW_e

highlight different control tasks in the boiler. The MVs and CVs of these cases 1−4 are shown in Table 2.

Case 1 focuses on the main steam parameters and the MW_e output, that is, the unit master control setup. Case 2 expands on the main steam temperature control task by also considering intermediate SH temperatures together with the unit master control. Case 3 centers on steam generation and combustion control by separating the "boiler load" MV into its individual flows. Case 4 combines all cases into a full plantwide boiler controllability and interaction analysis.

The power plant model was simulated for cases 1−4 in the open-loop around a 95% load level operating point. Stepwise ±5−10% changes were made to the chosen process inputs one at a time, with other inputs remaining constant. The open-loop gain matrix **G** (Table S1) between the MVs and CVs of the OTU-CFB could be determined from the settled output variable responses.

To outline ICI control structures with the PRG method, all possible MV−CV structures for a particular case were first analyzed with the steady-state RGA, Equation 2, and structures with negative RGA elements were discarded. The remaining solutions were screened by excluding candidates with negative NI values, eq 7. All possible PRG matrices were then calculated by closing loops down to 2 × 2 subsystems, eq 9, and applying eq 8. Structures with negative PRG elements were discarded. The remaining structures represented the ICI solutions, which were ranked based on their PRG elements (λ) in a similar way to the RGA (c.f. section 3.2.1):

$0 < \lambda \leq 0.1$	Bad: poor robustness and controllability, risk of singularity/negative PRG.
$0.1 < \lambda \leq 0.5$	Problematic: control issues, uncertainty with nonlinear PRG scale.
$0.5 < \lambda \leq 0.85$	Neutral: attention required during design, loops close → gains increase.
$0.85 < \lambda \leq 1.2$	Good: preferable, close to ideal PRG value with few interactions.
$1.2 < \lambda \leq 5$	Neutral: attention required during control, loops open → gains increase.
$5 < \lambda \leq 10$	Problematic: control issues, but not excessively large PRG.
$\lambda > 10$	Bad: poor performance with ill-conditioning or similar MV effects.

The steady-state PRG results were extended for multiple frequencies with the DRGA. The step test time series data was used to identify SISO transfer functions for all MV−CV pairs, using "tfest" in Matlab (least-squares minimization of weighted quadratic error, instrumental variable initialization). In most cases, second order models with delay were sufficient to capture the MV−CV dynamics (e.g., Figure 5). The frequency

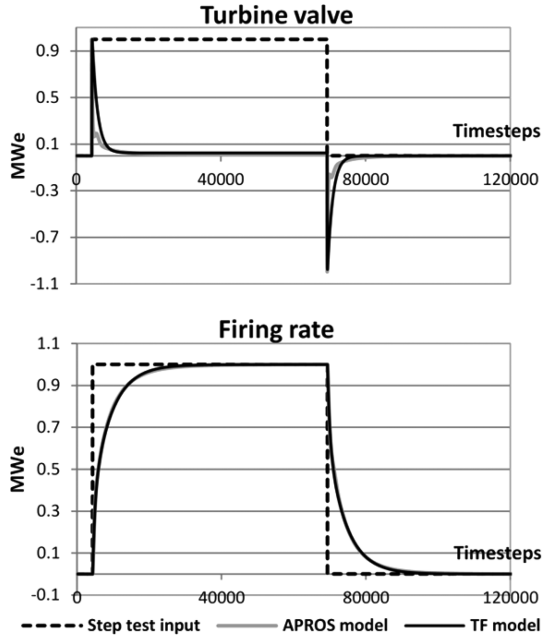

Figure 5. APROS simulator and 2nd order transfer function (TF) MW_e outputs (normalized) as a function of time for a positive and negative step test in the turbine valve and firing rate inputs.

responses of cases 1−4 were obtained using the transfer functions and eq 5 ("freqresp" in Matlab). The DRGA was then calculated for each frequency, eq 4. The focus was on both ICI and non-ICI structures in the 0−0.5 rad/s frequency range (e.g., Garrido et al.[24]), considering common boiler disturbance speeds (e.g., ≈ 3 s/MW_e load ramps).

In total, the OTU-CFB control structure selection procedure can be summarized as follows:

1. Select MVs and CVs, determine all possible MV−CV control structure candidates.
2. Make MV step tests, obtain process gain matrix **G** and MV−CV transfer functions.
3. Calculate RGA from **G** → discard structures with negative RGA elements.
4. Calculate NI index from **G** → discard structures with negative NI values.
5. Determine gain matrices $\bar{\mathbf{G}}_{mn}$ for all possible partially controlled subsystems.
6. Calculate PRG matrices for all partially controlled subsystems → Discard structures that have negative PRG elements in at least one subsystem.
7. Rank resulting ICI controllable structures based on their PRG element distribution (amounts of good and poor PRG elements in all partially controlled subsystems).
8. Calculate DRGA in desired ω range from transfer function frequency responses $\mathbf{H}(j\omega)$.
9. Rank preferred plantwide structures based on nDRGA at each frequency, compare to PRG.

DOI: 10.1021/acs.iecr.7b03259
Ind. Eng. Chem. Res. XXXX, XXX, XXX−XXX

5. OTU-CFB CONTROL STRUCTURE SELECTION

The outcomes of the relative gain analysis are explored here, the steady-state ICI PRG results in subsection 5.1 and the frequency domain DRGA results in subsection 5.2. The focus is on the conclusiveness of the steady-state analysis and the ICI criterion compared to the DRGA results.

5.1. Steady-State Analysis. All ICI control structures from the PRG analysis are displayed for cases 1−4 in sections 5.1.1−5.1.4. The RGA is also shown separately for case 1, while the RGAs of cases 2−4 are provided in the Supporting Information. Structures are annotated as vectors [a b c ...], where "a, b, c, ..." are the MV indices for controlling the respective CVs (Table 2), that is, the position in the vector is the CV and the number in that position is the MV. The structures with the largest amount of good (0.85−1.2) and smallest amount of poor PRG elements (<0.1 and >10) are ranked as the best.

5.1.1. Case 1: Main Control Loops. Case 1 examines the unit master control setup between the steam pressure and output MW_e, and how the loops interact with steam temperature control. In this 3 × 3 system, MVs and CVs can be paired into six possible control structures. Two MV−CV connections have negative RGA elements (Table 3), and three

Table 3. Steady-State RGA Matrix of the Case 1 System, 3 Input MVs and 3 Output CVs

RGA	MV →	T.valve	Tot DSH	Boiler load
CV ↓	INDEX	1	2	3
steam *p*	1	0.993	0.007	−0.0004
steam *T*	2	0.004	0.995	0.002
total MW_e	3	0.003	−0.002	0.999

structures thus remain: [1 2 3], [2 3 1], [2 1 3]. Notably, one of the negative RGA elements is "boiler load−steam pressure" (boiler-following control).

Control structures [1 2 3], [2 3 1], and [2 1 3] all have three partially controlled 2 × 2 subsystems [**1 2 3**] → [((1)) 2 3], [1 ((2)) 3], [1 2 ((3))]; [**2 3 1**]→ [((2)) 3 1], [2 ((3)) 1], [2 3 ((1))]; [**2 1 3**] → [((2)) 1 3], [2 ((1)) 3], [2 1 ((3))], closed loop marked with "(())". Each structure thus has six PRG elements from the remaining MV−CV connections (Table 4).

The three structures all have positive NI values, which directly make them ICI controllable (section 3.2.2). The ICI criterion thus provides no extra screening of structures compared to the RGA. The smallest degree of loop interactions (all PRG elements close to 1) is obtained with structure I, where the steam pressure is controlled with the turbine valve, the temperature is controlled with the spray water, and the generated MW_e is controlled with the boiler load. In the ICI structures ranked second and third, the pressure is controlled with the DSH flow, which is infeasible in practice. This is also visible as poor RGA and NI values. Structure III is clearly the worst in terms of the PRG.

Structure I represents basic turbine-following control. On the basis of the ICI criterion, this setup thus enables individual control loop tuning. This is understandable, as the output MW_e is ultimately determined by the generated heat, and the steam pressure can be directly adjusted with the turbine valve. In the basic boiler-following structure [3 2 1], the negative "boiler load−steam pressure" RGA element makes ICI controllability impossible. However, when this loop is closed to form a partially controlled system, the remaining control connections [((3)) 2 1] have excellent PRGs, meaning that this MV−CV connection is responsible for the poor controllability.

5.1.2. Case 2: Spray Water Flows. Superheater stage temperature control is considered by dividing the total DSH flow into its individual components DSH1, DSH2, and DSH3; 120 possible control connections exist for this 5 × 5 system. Only seven structures have positive RGA elements (Table S2), and one of these has a negative NI index. Three structures are ICI controllable based on the PRG (Table 5).

In structure I, the turbine valve is used for the steam pressure and each SH temperature is controlled with the preceding spray (DSH3 for main steam). The PRG distribution of structure I is clearly superior compared to structures II and III. The nine larger elements in structure I are all smaller than 1.9 and are generated in those subsystems, where the steam pressure and output MW_e loops are closed. In general, for all control structures the closing of these loops results in larger PRGs for the spray flow MVs. This points toward the similar effects of DSH1, DSH2, and DSH3 on the remaining process CVs, that is, the steam temperatures in the superheater line.

Structures II and III suggest that DSH1 should be used for steam pressure control and the turbine valve for the respective superheater temperature. A similar switch is suggested in structure III for DSH3 and the boiler load. These structures are impractical, and coincidentally these connections are also responsible for the poor PRG distributions of structures II and III.

5.1.3. Case 3: Combustion/Flue Gas Side. Analysis on the steam generation is provided by examining the fuel, primary/secondary air, and feedwater flows separately: 720 control structures can be generated in the resulting 6 × 6 system. Out of these, 28 have positive RGA elements (Table S3) and 19 have positive NI values.

Two ICI structures are obtained through the PRG analysis (Table 6). Both solutions are feasible in practice, but structure I is clearly superior in terms of its PRG distribution. Structure I corresponds to existing control practices: the fuel determines the heat generation, the feedwater has a direct effect on the evaporator, the secondary air is used for flue gas O_2 trim, and the primary oxidant has the largest cooling effect in the furnace. Structure II has a similar setup, but the roles of the feedwater and fuel MVs are reversed. The results thus highlight the

Table 4. Case 1 ICI Control Structures, Ranked by Their PRG distributions: Total Average (avg) PRG, Amounts of PRG Elements Belonging to Different Ranges, and NI Index

			no. of PRG elements in range							
rank	structure	NI	0−0.1	0.1−0.5	0.5−0.85	0.85−1.2	1.2−5	5−10	>10	avg. PRG
1	I: [1 2 3]	1.0089	0	0	0	6	0	0	0	1.00
2	II: [2 3 1]	82600	0	0	2	2	2	0	0	1.23
3	III: [2 1 3]	136	2	2	0	2	0	0	0	0.50

DOI: 10.1021/acs.iecr.7b03259
Ind. Eng. Chem. Res. XXXX, XXX, XXX−XXX

Table 5. Case 2 ICI Control Structures, Ranked by Their PRG Distributions: Total Average (avg) PRG, Amounts of PRG Elements Belonging to Different Ranges, and NI Index

			no. of PRG elements in range							
rank	structure	NI	0−0.1	0.1−0.5	0.5−0.85	0.85−1.2	1.2−5	5−10	>10	avg. PRG
1	I: [1 4 2 3 5]	0.340	0	0	0	61	9	0	0	1.11
2	II: [2 4 1 3 5]	18.7	14	3	12	33	8	0	0	0.77
3	III: [2 5 1 3 4]	11300	29	5	6	20	6	4	0	0.97

Table 6. Case 3 ICI Control Structures, Ranked by Their PRG Distributions: Total Average (avg) PRG, Amounts of PRG Elements Belonging to Different Ranges, and NI Index

			no. of PRG elements in range							
rank	structure	NI	0−0.1	0.1−0.5	0.5−0.85	0.85−1.2	1.2−5	5−10	>10	avg. PRG
1	I: [1 6 2 5 4 3]	0.231	0	0	1	117	62	0	0	1.33
2	II: [1 6 3 5 4 2]	1.60	30	26	21	65	38	0	0	0.95

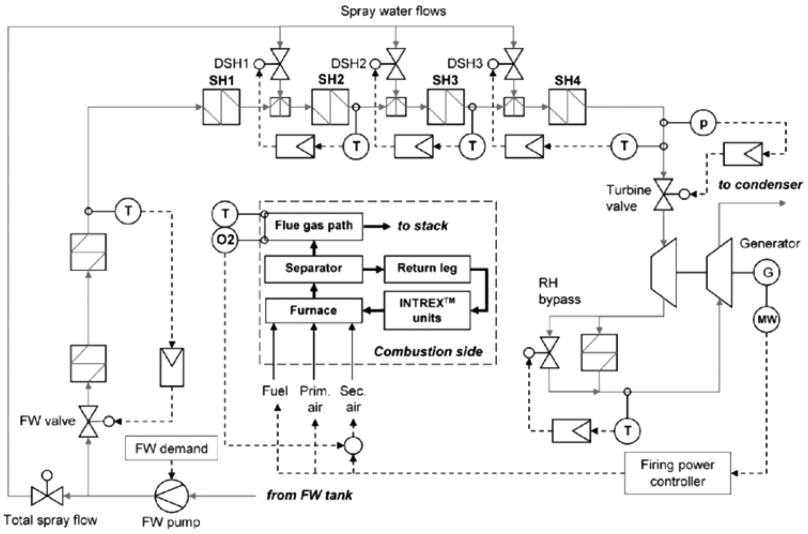

Figure 6. Conceptual plantwide control solution for the best ICI structure I of the PRG analysis. Dashed lines are control signals, exact controller or connection types are not considered.

Table 7. Case 4 ICI Control Structures, Ranked by Their PRG Distributions: Total Average (avg) PRG, Amounts of PRG Elements Belonging to Different Ranges, and NI Index

			no. of PRG elements in range							
rank	structure	NI	0−0.1	0.1−0.5	0.5−0.85	0.85−1.2	1.2−5	5−10	>10	avg. PRG
1	I: [1 6 2 3 4 5 7 8]	0.321	0	4	7	919	76	2	0	1.12
2	II: [1 6 7 3 4 5 2 8]	0.358	117	47	116	643	85	0	0	0.87
3	III: [1 6 8 3 4 5 7 2]	2.32	122	60	99	632	95	0	0	0.88

connection between the fuel and the feedwater as the main components for steam formation.

There are some larger PRG elements in structure I (>2, but not ill-conditioned), mostly related to the primary and secondary air flow control loops. The similar effects of the air flows on the flue gas O_2 and temperature CVs can thus be inferred from the analysis. Almost all of the 30 small (<0.1) PRG elements of structure II are related to the feedwater and fuel MV connections. The PRG thus highlights a preference between the two feasible ICI control structures: using the feedwater for MW_e control results in reduced controllability compared to the reverse solution.

5.1.4. Case 4: Overall OTU-CFB Control Structure. Case 4 examines the 8 × 8 plantwide problem. The primary air is assumed to be fixed to ensure fluidization; 40320 control structures exist between the MVs and CVs; 180 structures have no negative RGA elements (Table S4); and 94 solutions are left after the NI screening. The PRG analysis only produces three ICI structures and suggests that structure I (Figure 6) is clearly preferable, as it has a significant amount of excellent PRG values (Table 7). The two inferior structures II and III both have a large number of small PRG elements (over 100 elements below 0.1) that are mainly caused by pairings that are different from structure I. For each structure, 1008 PRG elements in 738 partially controlled systems were examined.

Structures I−III all contain some large PRG elements (>2) which are always observed for the DSH and feedwater flow control connections. This observation is similar to that in case 2, and the PRG thus suggests potential control performance issues caused by the similar effects of the DSH and feedwater flows on

DOI: 10.1021/acs.iecr.7b03259
Ind. Eng. Chem. Res. XXXX, XXX, XXX−XXX

superheater stage temperatures. The small PRG elements of the ICI structures (<0.5 for I and <0.1 for II and III) also show a surprising connection between feedwater flow and reheater control. The explanation might be that the chosen MV is the reheater bypass valve position, meaning that the bypass steam flow is also affected by feedwater flow changes.

The highest ranked plantwide structure I (Figure 6) corresponds to design experience for turbine-following control, meaning that the existing control practices can be validated as ICI, and controllers can be tuned individually without instability within this structure. This can be verified through simulations (Figure 7) by tuning each of the controllers of

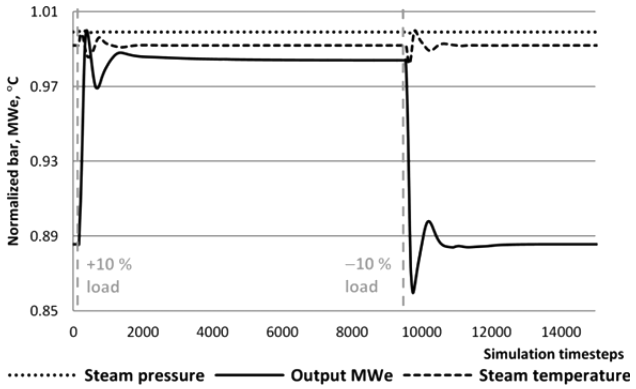

Figure 7. PID controlled constant pressure load step simulations with the original APROS boiler model (normalized), utilizing ICI control scheme I from Table 7 and Figure 6.

Figure 6 separately with all other control loops open, and then closing all loops to form the plantwide control system. On the basis of the simulations, the plantwide system remains stable as long as the individual loops are stable.

All in all, case 4 demonstrates that the PRG analysis can be used to synthesize ICI control structures for the full OTU-CFB flowsheet. The PRG provides a much more effective screening of control alternatives (3 solutions) in the large 8 × 8 system compared to the open-loop RGA (180 solutions), although the RGA suggests the same primary solution as the PRG. The RGA is more flexible than the PRG for enabling "unorthodox" control structures, but many of these would also be infeasible in practice (e.g., flue gas temperature control with steam side sprays).

5.2. Dynamic Analysis. All of the plantwide control structures that were suggested by the ICI analysis have a turbine-following unit master setup. Boiler-following MW_e control is enabled by the RGA and the NI in the 8 × 8 system (e.g., structure [2 6 8 3 4 5 7 1]), but not with the "firing power−steam pressure" control connection due to its negative RGA element. Adjusting the MW_e with the turbine valve is advantageous in real life for fast load transients, as having the TPM close to the product is better for control (cf. section 4.2.1). Transient speeds of the main MVs are listed in Table S5.

The unit master control findings from the ICI analysis can be explained by the small turbine valve static gain on the output MW_e (Figure 5), and by the conclusion that the boiler-following control loops are not independent in the ICI sense (no integrity). A change in the MW_e set point without compensating the firing power would require the valve position to change constantly, which would similarly decrease the steam pressure. This interaction becomes apparent when the boiler-following control structure [8 6 2 3 4 5 7 1] is analyzed further with the PRG. While the open-loop process has 143 PRGs below 0, closing the "firing power−steam pressure" loop (negative RGA) yields a subsystem that would fulfill all necessary ICI criteria (positive RGA, NI, and PRGs), even with a good PRG distribution. Therefore, as long as steam pressure control remains active, controllability could also be obtained for the boiler-following setup.

Hence, the ICI PRG analysis provides incomplete information about preferred OTU-CFB plantwide control structures. The process dynamic behavior also needs to be considered, as new loop interactions might be revealed, and MVs might have large transient effects compared to their steady-state gains. This is the motivation for the frequency-dependent DRGA investigations in sections 5.2.1−5.2.4. For simplicity, results are shown as DRGA numbers, nDRGA in eq 6.

5.2.1. Case 1: Main Control Loops. The DRGA numbers of ICI structures I−III (Table 4) and the basic boiler-following structure IV are shown in Figure 8. The turbine-following ICI structure I with the highest PRG element ranking also has the lowest nDRGA values for the whole frequency region. On the basis of the results, the DRGA validates the ICI structure I as the best option for the 3 × 3 system.

Boiler-following structure IV with its one negative RGA element at zero frequency has a lower nDRGA in the entire frequency region (excluding zero) than both of the ICI structures II and III. The degree of loop interactions also increases for the turbine-following structure I at higher frequencies, mainly due to the slowness of the "firing power−MW_e" control. The controllability of boiler-following structure IV similarly improves above zero, but its nDRGA starts to increase again above 0.15 rad/s because of the "turbine valve−steam pressure" DRGA, as the valve has an immediate effect on the steam pressure. Clearly the increased MW_e control performance of structure IV is overshadowed by the increased loop decoupling of structure I.

5.2.2. Case 2: Spray Water Flows. The DRGA (Figure 9) mostly suggests the same structure as the ICI analysis (Table 5). Structure I has the lowest DRGA number for almost the entire frequency range except for 0.05−0.1 rad/s, where boiler-following structure IV is momentarily preferred. In general, structure IV has the second lowest nDRGA at most frequencies, but it is infeasible at zero frequency.

The dynamic analysis thus does not emphasize boiler-following control, most likely since the "boiler load" MV includes both the fuel+air and feedwater flows. While the fuel and air affect the MW_e and steam pressure slowly, the feedwater alters the steam flow quickly (Table S5). This makes basic turbine-following control feasible even at higher frequencies.

On the basis of the individual DRGA elements, the temperatures at the turbine and after SH2 are clearly the best CV selections for DSH3 and DSH1. The preferred connection is less clear for DSH2 due to significant loop interactions. Interestingly, all structures show increased nDRGAs between 0.05−0.1 rad/s, which could indicate a problematic region for temperature disturbances.

5.2.3. Case 3: Combustion/Flue Gas Side. Several control structures beside ICI structures I−II (Table 6) can be considered in practice. The fuel, feedwater, air flow, and turbine valve MVs can, in principle, be used for controlling the steam pressure. Similarly, the evaporator temperature can be adjusted with the feedwater, air, or fuel flows. Either the fuel or the

DOI: 10.1021/acs.iecr.7b03259
Ind. Eng. Chem. Res. XXXX, XXX, XXX−XXX

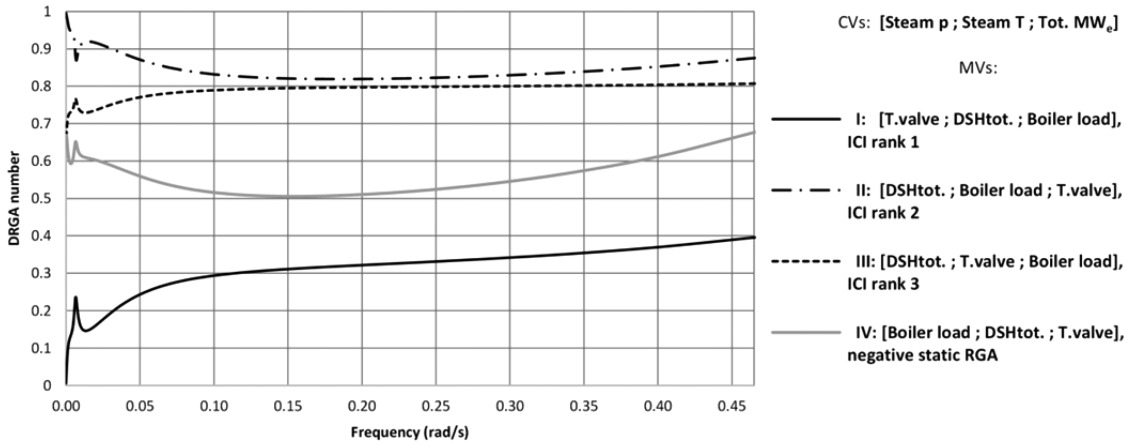

Figure 8. DRGA numbers as a function of frequency for case 1 control CV−MV connections: ICI structures I−III and boiler-following structure IV with negative zero frequency RGA.

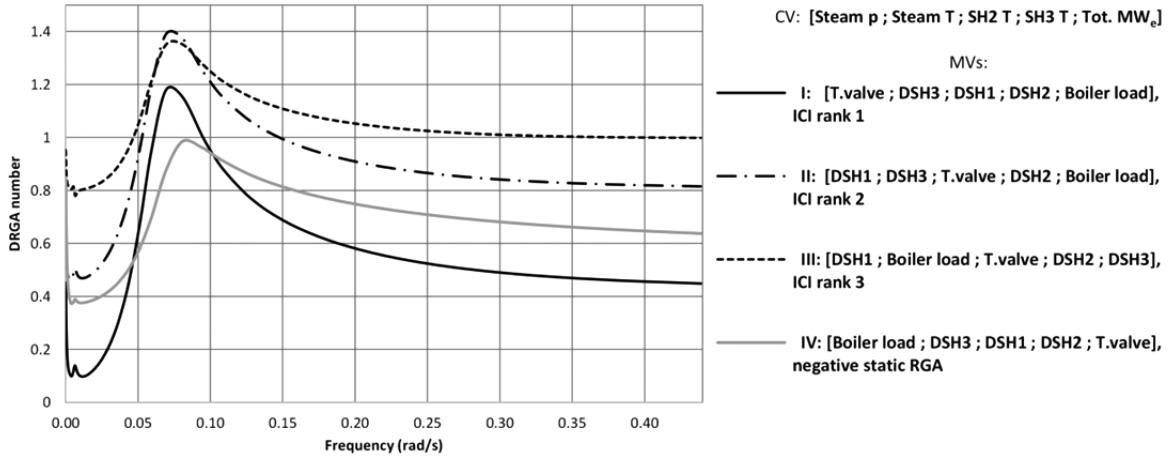

Figure 9. DRGA numbers as a function of frequency for case 2 control CV−MV connections: ICI structures I−III and boiler-following structure IV with negative zero frequency RGA.

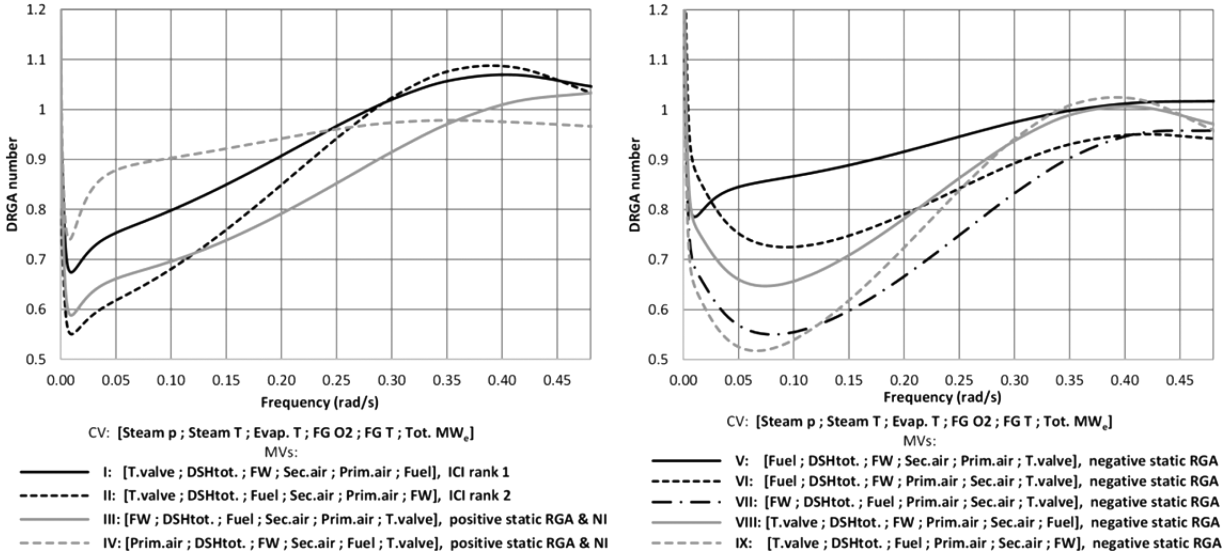

Figure 10. DRGA numbers as a function of frequency for case 3 control CV−MV connections: ICI structures I−II, structures III−IV with positive zero frequency RGA and NI, as well as boiler-following V−VII and turbine-following VIII−IX structures (negative zero frequency RGA).

primary air could be feasible for flue gas temperature control. Because of this, relevant non-ICI structures III−IX were included in the analysis (Figure 10).

Unlike the previous cases, there is a clear difference between the case 3 DRGA and ICI PRG results. ICI structure II immediately becomes better than the best ICI structure I beyond

DOI: 10.1021/acs.iecr.7b03259
Ind. Eng. Chem. Res. XXXX, XXX, XXX−XXX

zero frequency, and turbine-following structure IX has the lowest nDRGA between 0.02−0.12 rad/s. Above this range, boiler-following control (VI and VII) is preferable. These transitions between control structures take place because higher frequency disturbances favor connections that result in increased decoupling between the evaporator, the steam flow, and the turbine (Table 8). However, additional experiments also showed that the turbine-following setup IX became preferable again between 0.5−1 rad/s. For such fast disturbances, controlling the steam pressure with the MV that has the shortest settling time (Table S5) might indeed be preferable.

Table 8. Control Structures with the Lowest DRGA Numbers at Each Frequency Range in Case 3

freq (rad/s)	best structure	unit master setup	control structure change to decrease loop interactions
0−0.01	I	turbine-follow	ICI structure with independent loop tuning
0.01−0.02	II	turbine-follow	turbine−evaporator decoupling improved with "feedwater− MW_e" and "fuel−evaporator T" connections
0.02−0.12	IX	turbine-follow	primary and secondary air connections switched
0.12−0.4	VII	boiler-follow	boiler-follow control, MW_e controlled with feedwater
0.4−0.5	VI	boiler-follow	steam pressure and MW_e decoupling increased with "fuel− steam pressure", "feedwater−evaporator T" connections

A second observation is that the best control structures mostly apply a reversed oxidant control setup than what is used by ICI structures I and II, that is, the flue gas O_2 is controlled with the primary air and the flue gas temperature with the secondary air. This control structure change is interesting, especially when considering the negative values of these elements in Table S3.

5.2.4. Case 4: Plantwide Boiler Control. The control structures with the best DRGA numbers are given in Figure 11, including ICI structures I−III (Table 7) and relevant non-ICI structures IV−VI. Again, the best ICI structure I only has the lowest nDRGA at zero frequency. Above that, other structures are preferred.

Below 0.2 rad/s the lowest nDRGA is obtained with turbine-following ICI structure III, in which the feedwater is used for MW_e control and the firing power for the evaporator temperature. The boiler-following structure IV (steam pressure−feedwater control) also generates good nDRGA values. The basic boiler-following structure VI is clearly superior above 0.2 rad/s, and structure V also has low nDRGA values in this region. In V, the evaporator temperature is adjusted with DSH3 (infeasible), mainly due to the effect of the spray on the hotloop superheaters (Table S1).

The individual DRGA elements of the 8 × 8 system (Figure 12) show that DSH1 (d), DSH3 (f), and the reheater bypass valve (g) all have clear loop pairings (elements close to 1), as does the secondary air (c) below 0.25 rad/s. Inputs a, b, e, and h are more complex. The firing power (h) is mainly connected to the evaporation and combustion (flue gas O_2). Although the steam pressure was always selected as the CV for the turbine valve (a) by the steady-state ICI criterion, at 0.2−0.35 rad/s the valve is more suitable for MW_e control. The output MW_e is a good pairing for the feedwater (b), as is the steam pressure (low frequencies) and temperature (high frequencies). As in case 2, selecting a control pairing for DSH2 (e) is clearly challenging.

To conclude, no structure can be selected as superior in the entire frequency range based on the DRGA alone. An "optimal" solution would be a combination of turbine-following control for slow disturbances and boiler-following control for faster ones. These results can be verified through closed-loop simulations (PID control) for the "best" structures III and VI (Figure 13). The boiler-following structure VI can achieve an almost instantaneous MW_e response, but there is a significant interacting effect on the main steam pressure that can only be corrected slowly with the firing power, as indicated by the ICI analysis. Aggressive tuning for the pressure controller easily resulted in system instability, and the controllers had to be tuned together. Turbine-following ICI structure III on the other hand gives a slower MW_e response, but the related fluctuation in the steam pressure is small. The structure III loops are clearly less dependent on each other than in structure VI, and the control loops were easier to tune.

6. CONCLUSIONS

A once-through circulating fluidized bed boiler (OTU-CFB) was examined using relative gain analysis in order to form

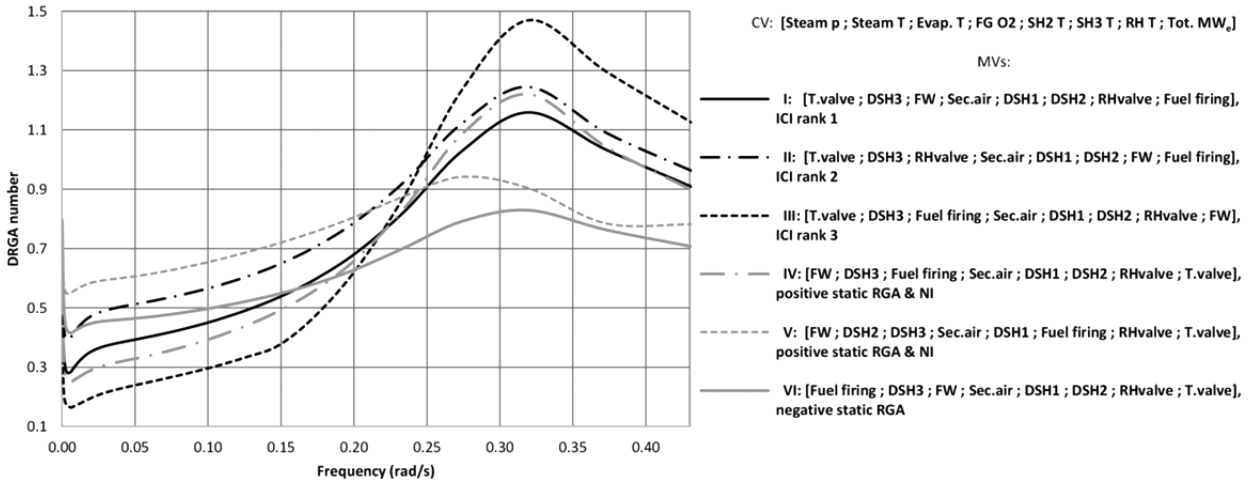

Figure 11. DRGA numbers as a function of frequency for case 4 control CV−MV connections: ICI structures I−III, structures IV−V with positive zero frequency RGA and NI, and the basic boiler-following structure VI with negative zero frequency RGA.

DOI: 10.1021/acs.iecr.7b03259
Ind. Eng. Chem. Res. XXXX, XXX, XXX−XXX

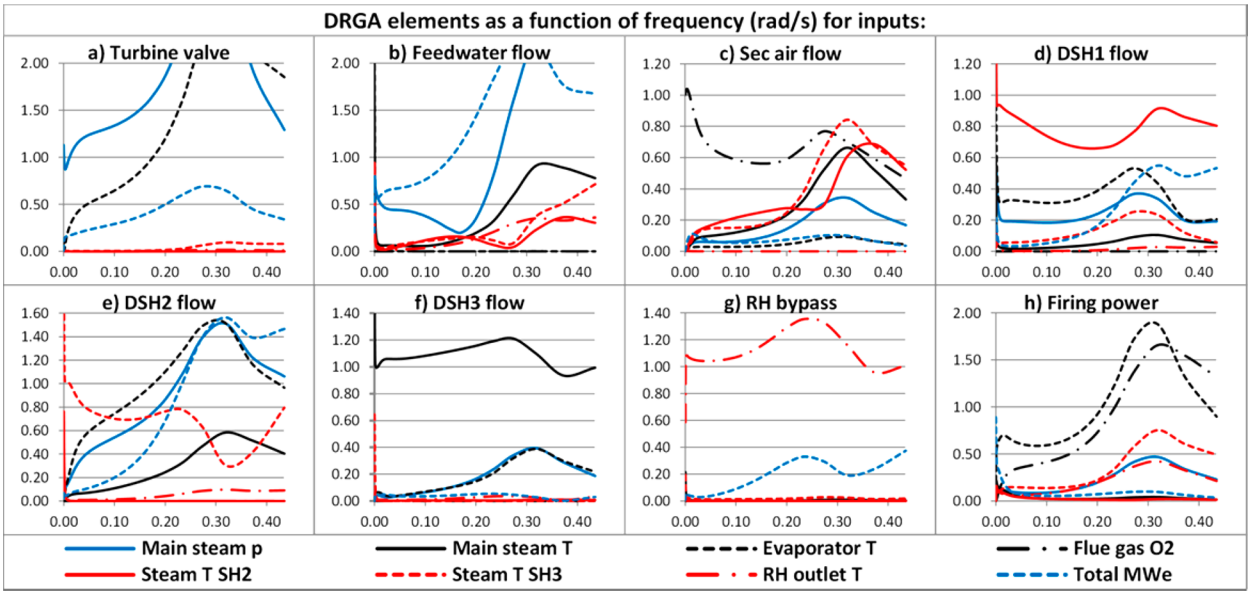

Figure 12. DRGA elements as a function of frequency for case 4; separate figures for each MV.

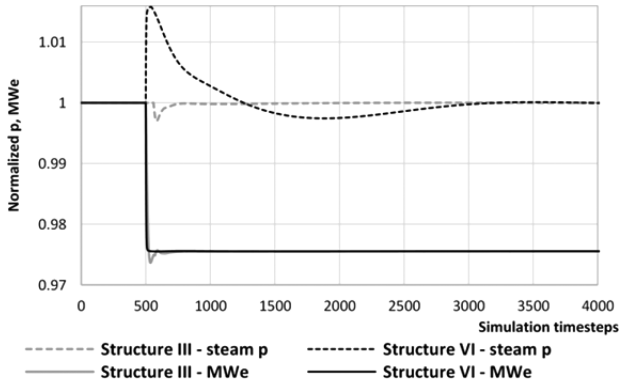

Figure 13. Normalized output MW_e set point step (constant pressure mode) for control structures III (turbine-following) and VI (boiler-following). PID controllers with tight tunings were used.

decentralized control structures for the power plant. The relative gain array (RGA) was applied to the steady-state gain matrix of an OTU-CFB simulator, as well as for higher frequencies (DRGA). Input−output sets ranging from 3 × 3 to 8 × 8 MIMO systems were investigated. Partial relative gain (PRG) was used to generate control structures with integral controllability with integrity (ICI). ICI is a useful property in the power plant, as it enables an independent tuning of its control loops. The PRG is only featured in a few publications.

The PRG ICI analysis provided a more rigorous screening of control structures than the RGA, especially for large OTU-CFB systems. The results were in line with existing control practices, using a basic turbine-following setup. However, the steady-state ICI criterion was also somewhat limited, as it labeled boiler-following control as infeasible despite its good real-life performance.

In contrast, control structures that were deemed to be poor at zero frequency often became favorable in the DRGA analysis, including boiler-following structures. Indeed, highly ranked ICI control structures commonly suffered from loop interactions above zero frequency. The findings are understandable for the turbine-following ICI structures, where fast output power disturbances are difficult to compensate. However, it should be noted that the chosen manipulated and controlled variable sets, as well as the frequency range, also influence the analysis outcomes.

The PRG and DRGA analysis highlighted the direct effect of the feedwater on the OTU steam path and the resulting interactions between steam pressure/temperature and output power control in the plantwide framework. The separate feedwater and spray flow inputs also cause slight ill-conditioning in the system. The DRGA indicated that turbine-following control would benefit from adjusting the output MW_e with the faster feedwater flow instead of the firing power.

Future work with OTU-CFB relative gain analysis will concern its broader application to the plantwide problem, considering multiple load levels, various disturbances and different process structures. Combustion power plants are facing major challenges in the near future, as they need to manage increasing response requirements in terms of speed and flexibility. It is likely that the layouts of future plants will differ from existing ones. The design of high-performing control structures thus requires that robust tools be available for plantwide control design.

■ ASSOCIATED CONTENT

Supporting Information

The Supporting Information is available free of charge on the ACS Publications website at DOI: 10.1021/acs.iecr.7b03259.

Table data: Open-loop gain matrix of the OTU-CFB process, RGA matrices of boiler test cases 2−4, time domain behavior of the main boiler manipulated variables (PDF)

■ AUTHOR INFORMATION

Corresponding Author

*Tel: +358443434979. E-mail: hultgrenmatias@gmail.com.

ORCID

Matias Hultgren: 0000-0001-8782-3808

Present Address

‡Outotec, Kuparitie 10, PO Box 69, FI-28101 Pori, Finland, matias.hultgren@outotec.com.

DOI: 10.1021/acs.iecr.7b03259
Ind. Eng. Chem. Res. XXXX, XXX, XXX−XXX

Notes

The authors declare no competing financial interest.

■ ACKNOWLEDGMENTS

The authors would like to acknowledge the industrial−academic cooperation between the University of Oulu and Sumitomo SHI FW Energy Oy (Varkaus, Finland). The work was partly supported by the Graduate School in Chemical Engineering (GSCE) doctoral program (Academy of Finland, Finnish Ministry of Education).

■ NOMENCLATURE

a = real term of CV−MV frequency response
b = imaginary term of CV−MV frequency response
CDOF = control degrees of freedom, −
DOF = degrees of freedom, −
DRGA = dynamic relative gain array, −
$\mathbf{G}$ = open-loop steady-state gain matrix between CVs and MVs
$\hat{\mathbf{G}}$ = modified $\mathbf{G}$, elements not used in control connections set to zero
$\bar{\mathbf{G}}_{mn}$ = partially controlled system $\mathbf{G}$, loops between m and n open (rest closed)
g = gain between CV and MV
$\mathbf{H}$ = open-loop frequency response matrix between CVs and MVs
$\mathbf{I}$ = identity matrix, −
m = controlled output variable (CV) index, −
n = manipulated input variable (MV) index, −
MW_e = output electrical megawatts, MW
N_X = amount of streams in DOF, X = "total"/"restrained"/"redundant", −
nDRGA = dynamic relative gain array number, −
NI = Niederlinski index, −
p = pressure, bar
PRG_{mn} = partial relative gain matrix, loops between m and n open (rest closed), −
RGA = relative gain array, −
T = temperature, °C
u = process input variable
y = process output variable
λ_{mn} = relative gain between CV m and MV n, −
ω = frequency, rad/s

■ REFERENCES

(1) Joronen, T.; Kovács, J.; Majanne, Y. *Voimalaitosautomaatio*; Suomen Automaatioseura ry: Helsinki, Finland, 2007.
(2) Klefenz, G. *Automatic Control of Steam Power Plants*; B.I.-Wissenschaftsverlag: Mannheim/Wien/Zürich, Germany/Austria/Switzerland, 1986.
(3) Sarkar, D. K. *Thermal Power Plant Design and Operation*; Elsevier: Amsterdam, Netherlands, 2015.
(4) Hultgren, M.; Ikonen, E.; Kovács, J. Oxidant control and air-oxy switching concepts for CFB furnace operation. *Comput. Chem. Eng.* **2014**, *61*, 203−219.
(5) Stanger, R.; Wall, T.; Spörl, R.; Paneru, M.; Grathwohl, S.; Weidmann, M.; Scheffknecht, G.; McDonald, D.; Myöhänen, K.; Ritvanen, J.; Rahiala, S.; Hyppänen, T.; Mletzko, J.; Kather, A.; Santos, S. Oxyfuel combustion for CO_2 capture in power plants. *Int. J. Greenhouse Gas Control* **2015**, *40*, 55−125.
(6) Leckner, B.; Gómez-Barea, A. Oxy-fuel combustion in circulating fluidized bed boilers. *Appl. Energy* **2014**, *125*, 308−318.
(7) Sharifzadeh, M. Integration of process design and control: A review. *Chem. Eng. Res. Des.* **2013**, *91* (12), 2515−2549.
(8) Luyben, W. L.; Tyréus, B. D.; Luyben, M. L. *Plantwide Process Control*; McGraw-Hill: New York, NY, 1999.
(9) Ogunnaike, B. A.; Ray, W. H. *Process Dynamics, Modeling, and Control*; Oxford University Press: New York, NY, Oxford, U.K., 1994.
(10) Skogestad, S.; Postlethwaite, I. *Multivariable Feedback Control, Analysis and Design*; Wiley: Chichester, U.K., 1996.
(11) McAvoy, T. J. Some Results on Dynamic Interaction Analysis of Complex Control Systems. *Ind. Eng. Chem. Process Des. Dev.* **1983**, *22* (1), 42−49.
(12) Bristol, E. H. On a new measure of interaction for multivariable process control. *IEEE Trans. Autom. Control* **1966**, *11* (1), 133−134.
(13) Witcher, M.; McAvoy, T. J. Interacting control systems: steady state and dynamic measurement of interaction. *ISA Trans.* **1977**, *16*, 35−41.
(14) Häggblom, K. E. In *Partial Relative Gain: A New Tool for Control Structure Selection*. Proceedings of the 1997 AIChE Annual Meeting, Los Angeles, CA, Nov 16−21, 1997; Los Angeles, 1997.
(15) Campo, P. J.; Morari, M. Achievable Closed-Loop Properties of Systems Under Decentralized Control: Conditions Involving the Steady-State Gain. *IEEE Trans. Autom. Control* **1994**, *39* (5), 932−943.
(16) Chiu, M.-S.; Arkun, Y. Decentralized Control Structure Selection Based on Integrity Considerations. *Ind. Eng. Chem. Res.* **1990**, *29* (3), 369−373.
(17) Niva, L.; Ikonen, E.; Kovács, J. Self-optimizing control structure design in oxy-fuel circulating fluidized bed combustion. *Int. J. Greenhouse Gas Control* **2015**, *43*, 93−107.
(18) Skogestad, S. Control structure design for complete chemical plants. *Comput. Chem. Eng.* **2004**, *28* (1−2), 219−234.
(19) Prasad, G.; Irwin, G. W.; Swidenbank, E.; Hogg, B. W. Plant-wide predictive control for a thermal power plant based on a physical plant model. *IEE Proc.: Control Theory Appl.* **2000**, *147* (5), 523−537.
(20) Garduno-Ramirez, R.; Lee, K. Y. Compensation of control-loop interaction for power plant wide-range operation. *Control Eng. Pract.* **2005**, *13* (12), 1475−1487.
(21) Aurora, C.; Magni, L.; Scattolini, R.; Colombo, P.; Pretolani, F.; Villa, G. Predictive control of thermal Power Plants. *Int. J. Robust Nonlin. Control* **2004**, *14* (4), 415−433.
(22) Biyanto, T. R.; Prasetya, H. E. G.; Bayuaji, R.; Nugroho, G.; Soehartanto, T. Design Plant-wide Control to Waste Heat Recovery Generation on Cement Industry Based HYSYS. *Procedia Comput. Sci.* **2015**, *72*, 170−177.
(23) Rambalee, P.; Gous, G.; de Villiers, P. G. R.; McCulloch, N.; Humphries, G. In *Control and Stabilization of a Multiple Boiler Plant: An APC Approach*. Proceedings of the 13th IFAC Symposium on Automation in Mining, Mineral and Metal Processing, Cape Town, South Africa, Aug 2−4, 2010; Jemwa, G. T., Aldrich, C., Eds.; IFAC: Cape Town, 2010; pp 109−114.
(24) Garrido, J.; Morilla, F.; Vázquez, F. In *Centralized PID control by decoupling of a boiler-turbine unit*. Proceedings of the 2009 European Control Conference, Budapest, Hungary, Aug 23−26, 2009; Budapest, 2009; pp 4007−4012.
(25) Manousiouthakis, V.; Savage, R.; Arkun, Y. Synthesis of Decentralized Process Control Structures Using the Concept of Block Relative Gain. *AIChE J.* **1986**, *32* (6), 991−1003.
(26) Basu, P. *Combustion and Gasification in Fluidized Beds*; Taylor & Francis: Boca Raton, FL, 2006.
(27) Blaszczuk, A.; Nowak, W.; Krzywanski, J. Effect of bed particle size on heat transfer between fluidized bed of group b particles and vertical rifled tubes. *Powder Technol.* **2017**, *316*, 111−122.
(28) Kovács, J.; Kettunen, A.; Ojala, J. In *Modelling and control design of once-through boilers*. Proceedings of the 8th Power Plant and Power System Control Symposium, Toulouse, France, Sept 2−5, 2012; Fadel, M., Caux, S., Eds.; IFAC: Toulouse, 2012; pp 196−200.
(29) Paloranta, M.; Kettunen, A.; Kovács, J. In *Dynamic simulations of the World's first supercritical CFB-OTU boiler*. Proceedings of the 9th International Conference on Circulating Fluidized Beds, Hamburg, Germany, May 13−16, 2008; Hamburg, 2008.

DOI: 10.1021/acs.iecr.7b03259
Ind. Eng. Chem. Res. XXXX, XXX, XXX−XXX

(30) Blaszczuk, A.; Nowak, W.; Jagodzik, S. Effects of operating conditions on deNO$_x$ system efficiency in supercritical circulating fluidized bed boiler. *J. Power Technol.* **2013**, *93* (1), 1−8.
(31) Duan, L.; Zhao, C.; Zhou, W.; Qu, C.; Chen, X. O_2/CO_2 coal combustion characteristics in a 50 kW_{th} circulating fluidized bed. *Int. J. Greenhouse Gas Control* **2011**, *5* (4), 770−776.
(32) Krzywanski, J.; Czakiert, T.; Blaszczuk, A.; Rajczyk, R.; Muskala, W.; Nowak, W. A generalized model of SO_2 emissions from large- and small-scale CFB boilers by artificial neural network approach: Part 1. The mathematical model of SO_2 emissions in air-firing, oxygen-enriched and oxycombustion CFB conditions. *Fuel Process. Technol.* **2015**, *137*, 66−74.
(33) Ritvanen, J.; Kovács, J.; Salo, M.; Hultgren, M.; Tourunen, A.; Hyppänen, T. In *1-D Dynamic Simulation Study of Oxygen Fired Coal Combustion in Pilot and Large Scale CFB Boilers*. Proceedings of the 21st International Conference on Fluidized Bed Combustion, Vol. 1, Naples, Italy, June 3−6, 2012; EnzoAlbanoEd.e: Naples, 2012; pp 72−79.
(34) Hultgren, M.; Ikonen, E.; Kovács, J. In *Circulating Fluidized Bed Boiler State Estimation with an Unscented Kalman Filter Tool*. Proceedings of the 23rd IEEE International Conference on Control Applications, Antibes, France, Oct 8−10, 2014; pp 310−315.
(35) Stephanopoulos, G.; Ng, C. Perspectives on the synthesis of plant-wide control structures. *J. Process Control* **2000**, *10* (2−3), 97−111.
(36) Luyben, W. L. Design and Control Degrees of Freedom. *Ind. Eng. Chem. Res.* **1996**, *35* (7), 2204−2214.
(37) Konda, N. V. S. N. M.; Rangaiah, G. P.; Krishnaswamy, P. R. A simple and effective procedure for control degrees of freedom. *Chem. Eng. Sci.* **2006**, *61* (4), 1184−1194.
(38) Price, R. M.; Georgakis, C. Plantwide regulatory control design procedure using a tiered framework. *Ind. Eng. Chem. Res.* **1993**, *32* (11), 2693−2705.
(39) Price, R. M.; Lyman, P. R.; Georgakis, C. Throughput Manipulation in Plantwide Control Structures. *Ind. Eng. Chem. Res.* **1994**, *33* (5), 1197−1207.
(40) Ogata, K. *Modern Control Engineering*, 5th ed.; Prentice Hall: New Jersey, NJ, 2010.
(41) Shields, R. W.; Pearson, J. B. Structural Controllability of Multiinput Linear Systems. *IEEE Trans. Autom. Control* **1976**, *21* (2), 203−212.
(42) Xiong, Q.; Cai, W.-J.; He, M.-J. A practical loop pairing criterion for multivariable processes. *J. Process Control* **2005**, *15* (7), 741−747.
(43) Chang, J.-W.; Yu, C.-C. The relative gain for non-square multivariable systems. *Chem. Eng. Sci.* **1990**, *45* (5), 1309−1323.
(44) Alhammadi, H. Y.; Romagnoli, J. A. Process design and operation: Incorporating environmental, profitability, heat integration and controllability considerations. In *The Integration of Process Design and Control*; Seferlis, P., Georgiadis, M. C., Eds.; Elsevier: Amsterdam, Netherlands, 2004; pp 264−305.
(45) Skogestad, S.; Morari, M. Implications of Large RGA Elements on Control Performance. *Ind. Eng. Chem. Res.* **1987**, *26* (11), 2323−2330.
(46) Skogestad, S. Dynamics and Control of Distillation Columns: A Tutorial Introduction. *Chem. Eng. Res. Des.* **1997**, *75* (6), 539−562.
(47) Laub, A. J. Efficient Multivariable Frequency Response Computations. *IEEE Trans. Autom. Control* **1981**, *26* (2), 407−408.
(48) Engell, S.; Trierweiler, J. O.; Völker, M.; Pegel, S. Tools and indices for dynamic I/O- controllability assessment and control structure selection. In *The Integration of Process Design and Control*; Seferlis, P., Georgiadis, M. C., Eds.; Elsevier: Amsterdam, Netherlands, 2004; pp 430−463.
(49) Apros Process Simulation Software, Nuclear and Thermal Power Plant Applications. Fortum Power and Heat Oy & VTT Technical Research Centre of Finland Ltd. http://www.apros.fi (accessed Sept 19, 2017).
(50) Hänninen, M.; Ylijoki, J. *The one-dimensional separate two-phase flow model of APROS, VTT Tiedotteita—Research Notes 2443*; Technical Report, VTT Technical Research Centre of Finland; Edita Prima Oy: Helsinki, Finland, 2008.

DOI: 10.1021/acs.iecr.7b03259
Ind. Eng. Chem. Res. XXXX, XXX, XXX−XXX